

Transfer of energy in the variational multiscale formulation of LES

By A. A. Oberai †, V. Gravemeier AND G. C. Burton

The transfer of energy from the resolved scales to the subgrid scales in homogeneous isotropic turbulence is studied, within the context of the variational formulation of large eddy simulation. In particular, the relative contributions to this transfer from the coarse and the fine resolved scales are evaluated and their dependence on the choice of an ideal LES solution is examined. It is found that when the L_2 projection of the DNS solution onto a truncated Fourier space is selected as the ideal LES solution, the energy transfer from the fine resolved scales is the dominant contribution. On the other hand, when the ideal LES solution is defined to be the nodal interpolant of the DNS solution on a coarse finite element mesh, contributions from both the coarse and the fine resolved scales are important. These observations are made by performing *a-priori* analysis using a DNS database and are also explained using an analytical theory of turbulence closure. These results indicate that within the variational formulation of LES, the definition of a “good model” is closely tied to the choice of the ideal LES solution, which in turn is dependent on the function spaces utilized in solving the problem.

1. Introduction

The variational multiscale (VMS) formulation for large eddy simulation (LES) of turbulent flows (Hughes, Mazzei & Jansen 2000; Collis 2001) differs from the filtered formulation in that models are introduced in the weak form of the Navier Stokes equations and are used to account for the approximation of infinite-dimensional function spaces by their finite-dimensional counterparts. Another feature of the VMS formulation is that different models are introduced in the equations for the coarse and the fine resolved scales. In most applications to date, no model has been used in the coarse scale equations and the Smagorinsky model has been used in the fine scale equations (see for example Hughes, Oberai & Mazzei 2001). In a spectral discretization, this choice is easily motivated by the characteristics of the spectral eddy viscosity, which is small for low wavenumbers and large for wavenumbers close to the cutoff.

A closer look at the VMS formulation reveals that the choice of an ideal model is closely linked to the choice of what constitutes an ideal LES solution, which in turn depends on the basis used to solve the problem. Hence what might be a good model when using a spectral basis (say Fourier modes) may not be a good model for a typical finite element basis. This observation has an analog in the filtered LES formulation, where ideal models (in terms of predicting the right energy transfer) for a sharp cutoff filter and a Gaussian filter are very different (see for example Leslie & Quarini 1979; Cerutti, Meneveau, & Knio 2000). With this in mind we explore in this manuscript what constitutes an ideal model (in terms of multiscale transfer of energy) for the VMS formulation, for different definitions of ideal LES solutions. We use DNS data to perform our analysis and thereafter

† Department of Aerospace and Mechanical Engineering, Boston University.

explain our results using analytical theories of turbulence. We consider two different ideal LES solutions. The first corresponds to the Fourier truncation of the DNS solution onto a smaller space. The second corresponds to the nodal interpolant of the DNS solution on a coarse grid constructed using typical finite element basis. Through our investigations we conclude that the scale dependence of the transfer of energy to the subgrid scales for these two ideal LES solutions is significantly different.

2. Variational Model and an Ideal LES Model

2.1. Strong and Weak Forms

We consider the motion of an incompressible fluid in $Q = \Omega \times]T_1, T_2[$, where $\Omega = [0, 2\pi]^3$ is the spatial domain and $]T_1, T_2[$ is the time period of interest. The strong form of the problem is given by

$$\mathbf{u}_{,t} + \nabla \cdot (\mathbf{u} \otimes \mathbf{u}) + \nabla p - \nu \nabla^2 \mathbf{u} = \mathbf{f}, \text{ in } Q \quad (2.1)$$

$$\nabla \cdot \mathbf{u} = 0, \text{ in } Q. \quad (2.2)$$

In the above equations \mathbf{u} is the fluid velocity field and p is the pressure, ν is the kinematic viscosity and the symbol \otimes denotes the outer product of two vectors. In addition, since we are restricting our analysis to homogeneous isotropic turbulence, we assume that the solution satisfies periodic boundary conditions.

We consider a weak or a variational formulation of the Navier Stokes equations (see for example Foias, Manley, Rosa & Temam 2001) given by: Find $\mathbf{U}(\cdot, t) = [\mathbf{u}(\cdot, t), p(\cdot, t)]^T \in \mathcal{V}$, such that

$$B(\mathbf{W}, \mathbf{U}) = (\mathbf{W}, \mathbf{F}), \quad \forall \mathbf{W} = [\mathbf{w}, q]^T \in \mathcal{V}, \forall t \in]T_1, T_2[, \quad (2.3)$$

where the semi-linear form $B(\cdot, \cdot)$ is defined as

$$B(\mathbf{W}, \mathbf{U}) = (\mathbf{w}, \mathbf{u}_{,t}) - (\nabla \mathbf{w}, \mathbf{u} \otimes \mathbf{u}) + (\mathbf{w}, \nabla p) + 2\nu(\nabla^S \mathbf{w}, \nabla^S \mathbf{u}) - (\nabla q, \mathbf{u}), \quad (2.4)$$

and where

$$(\mathbf{W}, \mathbf{F}) = (\mathbf{w}, \mathbf{f}). \quad (2.5)$$

Throughout this text (\cdot, \cdot) is used to denote the L_2 inner product.

The infinite dimensional function space \mathcal{V} is defined as

$$\mathcal{V} = \left\{ \mathbf{V} = [\mathbf{v}, r]^T \mid \mathbf{v} \in H^1(\Omega); r \in L_2(\Omega) \right\}. \quad (2.6)$$

In the equation above $H^1(\Omega)$ denotes the Sobolev space of vector-valued functions that are square-integrable and whose derivatives are also square-integrable. This implies that the energy and the enstrophy of the weak solutions remain finite. $L_2(\Omega)$ denotes the space of scalar functions that are square integrable. In addition, we assume that the periodic boundary conditions (though not explicitly stated) are built into the definition of \mathcal{V} .

Let $\mathcal{V}^h \subset \mathcal{V}$ be a finite dimensional subspace. Note that since \mathcal{V}^h is a subspace of \mathcal{V} , (2.3) implies that the exact solution \mathbf{U} satisfies

$$B(\mathbf{W}^h, \mathbf{U}) = (\mathbf{W}^h, \mathbf{F}), \quad \forall \mathbf{W}^h \in \mathcal{V}^h, \forall t \in]T_1, T_2[. \quad (2.7)$$

The Galerkin method when applied to (2.3) yields the following equation for the approximate solution \mathbf{U}^h . Find $\mathbf{U}^h(\cdot, t) \in \mathcal{V}^h$, such that

$$B(\mathbf{W}^h, \mathbf{U}^h) = (\mathbf{W}^h, \mathbf{F}), \quad \forall \mathbf{W}^h \in \mathcal{V}^h, \forall t \in]T_1, T_2[. \quad (2.8)$$

2.2. Ideal LES Model

The Galerkin solution essentially corresponds to a Direct Numerical Simulation (DNS) of the original problem. It is well known that if the space \mathcal{V}^h is unable to represent the large inertial scales of motion as well as the fine dissipative scales, the Galerkin solution will be inaccurate. In particular, it will be corrupted by an unphysical pile up of energy at the finest resolved scales. This solution may be improved upon by adding a model term to the Galerkin approximation. This leads to the following variational equation, which we shall refer to as the modeled equation: Find $\mathbf{U}^h(\cdot, t) \in \mathcal{V}^h$, such that

$$B(\mathbf{W}^h, \mathbf{U}^h) + M(\mathbf{W}^h, \mathbf{U}^h; h, \mathbf{c}) = (\mathbf{W}^h, \mathbf{F}), \quad \forall \mathbf{W}^h \in \mathcal{V}^h, \forall t \in]T_1, T_2[. \quad (2.9)$$

In (2.9), $M(\mathbf{W}^h, \mathbf{U}^h; h, \mathbf{c})$ is the model term that is linear in \mathbf{W}^h and non-linear in \mathbf{U}^h . It also depends on the mesh size h and a vector of parameters \mathbf{c} . Note that due to the presence of the model, the solution of (2.9) and the Galerkin solution are distinct, even though they are represented by the same \mathbf{U}^h in our development.

We now introduce the concept of an optimal solution in the space \mathcal{V}^h . For this we define a *restriction operator* $\mathcal{P}^h : \mathcal{V} \rightarrow \mathcal{V}^h$, such that $\mathcal{P}^h \mathbf{U} \in \mathcal{V}^h$ is the optimal representation of \mathbf{U} in \mathcal{V}^h . For example, $\mathcal{P}^h \mathbf{U}$ may be the nodal interpolant or a suitable projection (L_2 or H^1 in our case) of \mathbf{U} in \mathcal{V}^h , in which case \mathcal{P}^h will be the interpolation or the projection operator, respectively. We would like to select our model term in (2.9) such that the solution \mathbf{U}^h is optimal. Thus requiring $\mathbf{U}^h = \mathcal{P}^h \mathbf{U}$ in (2.9) we have

$$M(\mathbf{W}^h, \mathcal{P}^h \mathbf{U}; h, \mathbf{c}) = (\mathbf{W}^h, \mathbf{F}) - B(\mathbf{W}^h, \mathcal{P}^h \mathbf{U}), \quad \forall \mathbf{W}^h \in \mathcal{V}^h, \forall t \in]T_1, T_2[. \quad (2.10)$$

Using (2.7) in (2.10) we arrive at

$$M(\mathbf{W}^h, \mathcal{P}^h \mathbf{U}; h, \mathbf{c}) = B(\mathbf{W}^h, \mathbf{U}) - B(\mathbf{W}^h, \mathcal{P}^h \mathbf{U}), \quad \forall \mathbf{W}^h \in \mathcal{V}^h, \forall t \in]T_1, T_2[. \quad (2.11)$$

This equation defines the model required to generate the optimal solution. The net energy transferred by the ideal model to the subgrid scales is obtained by setting $\mathbf{W}^h = \mathbf{V}^h \equiv \mathcal{P}^h[\mathbf{u}, 0]^T$ in the above equation and is given by

$$T^h \equiv M(\mathbf{V}^h, \mathcal{P}^h \mathbf{U}; h, \mathbf{c}) = B(\mathbf{V}^h, \mathbf{U}) - B(\mathbf{V}^h, \mathcal{P}^h \mathbf{U}). \quad (2.12)$$

In this study we wish to estimate the scale dependence of this energy transfer. In other words we wish to quantify the proportion of the total transfer from the coarse and the fine resolved scales in \mathcal{V}^h . For this purpose we split \mathcal{V}^h as follows

$$\mathcal{V}^h = \bar{\mathcal{V}}^h \oplus \acute{\mathcal{V}}^h, \quad (2.13)$$

and likewise split \mathbf{V}^h as

$$\mathbf{V}^h = \bar{\mathbf{V}}^h + \acute{\mathbf{V}}^h, \quad (2.14)$$

where $\bar{\mathbf{V}}^h \in \bar{\mathcal{V}}^h$ represents the coarse resolved scales and $\acute{\mathbf{V}}^h \in \acute{\mathcal{V}}^h$ represents the fine resolved scales. Now the net transfer of energy due to the model can be split into a coarse and a fine scale part such that

$$T^h = \bar{T}^h + \acute{T}^h, \quad (2.15)$$

where

$$\bar{T}^h \equiv M(\bar{\mathbf{V}}^h, \mathcal{P}^h \mathbf{U}; h, \mathbf{c}) = B(\bar{\mathbf{V}}^h, \mathbf{U}) - B(\bar{\mathbf{V}}^h, \mathcal{P}^h \mathbf{U}), \quad (2.16)$$

$$\acute{T}^h \equiv M(\acute{\mathbf{V}}^h, \mathcal{P}^h \mathbf{U}; h, \mathbf{c}) = B(\acute{\mathbf{V}}^h, \mathbf{U}) - B(\acute{\mathbf{V}}^h, \mathcal{P}^h \mathbf{U}). \quad (2.17)$$

In the following section, using the DNS data, we will compute the ratios \bar{T}^h/T^h and \hat{T}^h/T^h when the function space \mathcal{V}^h is constructed from Fourier modes and typical finite element shape functions.

The above equations represent the ‘‘ideal’’ transfer of energy. We will also compare this transfer to the transfer predicted by the Smagorinsky model (Smagorinsky 1963). The Smagorinsky transfer is given by is given by

$$\bar{T}_{\text{smag}}^h \equiv M_{\text{smag}}(\bar{\mathbf{V}}^h, \mathcal{P}^h \mathbf{U}; h, \mathbf{c}) \quad (2.18)$$

$$\hat{T}_{\text{smag}}^h \equiv M_{\text{smag}}(\hat{\mathbf{V}}^h, \mathcal{P}^h \mathbf{U}; h, \mathbf{c}), \quad (2.19)$$

where the Smagorinsky term is defined as

$$M_{\text{smag}}(\mathbf{W}, \mathbf{U}; h, \mathbf{c}) = 2(ch)^2 (\nabla^S \mathbf{w}, |\nabla^S \mathbf{u}| \nabla^S \mathbf{u}). \quad (2.20)$$

3. Numerical Results

In this section we present the numerical results of our *a-priori* analysis. The DNS solution used in our analysis is the solution to a forced, homogeneous, isotropic problem with $Re_\lambda = 168$ (see Jimenez, Wray, Saffman & Rogallo 1993 for details).

3.1. Spectral Basis

We expand the DNS solution and its restrictions to the finite dimensional spaces using Fourier modes. We approximate \mathcal{V} with the space spanned by Fourier modes with wavenumber less than k_c . Note that $k_c > k_d$, the dissipation wavenumber, so that \mathcal{V} which is infinite dimensional may be accurately represented by this finite dimensional space. The space \mathcal{V}^h is also spanned by Fourier modes, but with wavenumbers less than k_c^h where $k_c^h \ll k_d$. The restriction operator \mathcal{P}^h is the L_2 projection of \mathcal{V} onto \mathcal{V}^h . As a result

$$\mathbf{U}(\mathbf{x}) = \sum_{k \leq k_c} \hat{\mathbf{U}}(\mathbf{k}) e^{i\mathbf{k} \cdot \mathbf{x}} = \sum_{k \leq k_c} [\hat{\mathbf{u}}(\mathbf{k}), \hat{p}(\mathbf{k})]^T e^{i\mathbf{k} \cdot \mathbf{x}} \quad (3.1)$$

$$\mathcal{P}^h \mathbf{U}(\mathbf{x}) = \sum_{k \leq k_c^h} \hat{\mathbf{U}}(\mathbf{k}) e^{i\mathbf{k} \cdot \mathbf{x}} = \sum_{k \leq k_c^h} [\hat{\mathbf{u}}(\mathbf{k}), \hat{p}(\mathbf{k})]^T e^{i\mathbf{k} \cdot \mathbf{x}} \quad (3.2)$$

$$\mathbf{V}^h(\mathbf{x}) = \sum_{k \leq k_c^h} \hat{\mathbf{V}}(\mathbf{k}) e^{i\mathbf{k} \cdot \mathbf{x}} = \sum_{k \leq k_c^h} [\hat{\mathbf{u}}(\mathbf{k}), 0]^T e^{i\mathbf{k} \cdot \mathbf{x}}, \quad (3.3)$$

where $k = |\mathbf{k}|$. For this study we choose $k_c = 256$ and $k_c^h = 32$.

In order to compute the multiscale transfer of energy we define $\bar{\mathcal{V}}^h$ to be the space spanned by Fourier modes with wavenumbers less than $k_c^h/2 = 16$. Thus

$$\bar{\mathbf{V}}^h(\mathbf{x}) = \sum_{k \leq k_c^h/2} \hat{\mathbf{V}}(\mathbf{k}) e^{i\mathbf{k} \cdot \mathbf{x}} = \sum_{k \leq k_c^h/2} [\hat{\mathbf{u}}(\mathbf{k}), 0]^T e^{i\mathbf{k} \cdot \mathbf{x}} \quad (3.4)$$

$$\hat{\mathbf{V}}^h(\mathbf{x}) = \mathbf{V}^h(\mathbf{x}) - \bar{\mathbf{V}}^h(\mathbf{x}). \quad (3.5)$$

Using (3.1), (3.2), (3.4) and (3.5) in (2.16) and (2.17) we compute the energy transfer from the coarse and fine resolved scales. We note that due to the properties of the restriction operator and the Fourier modes, there is no contribution to the energy transfer from the linear terms. The values of the multiscale transfers are reported in the first column of Table 1. We observe that the energy transfer to the subgrid scales exclusively from the

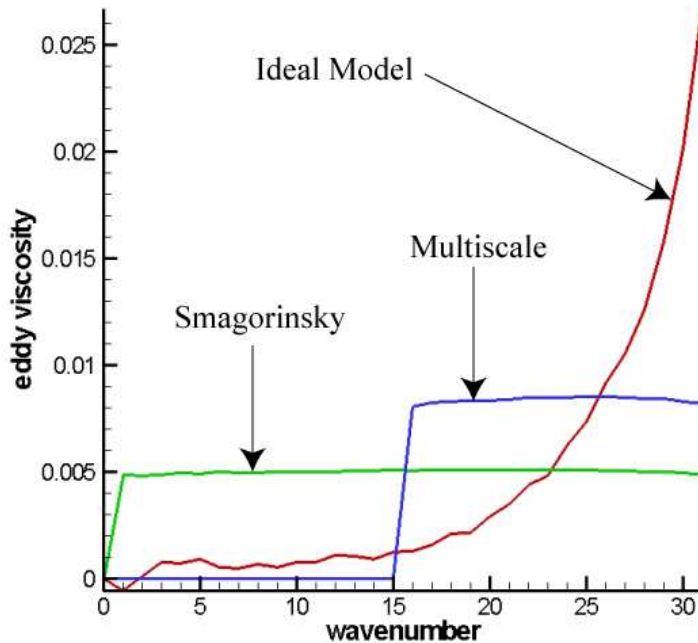


FIGURE 1. Spectral eddy viscosity as a function of wavenumber (results obtained using DNS database). Results for the Ideal model, the Smagorinsky model and the variational multiscale approach are shown. Viscosities are scaled such that the total energy transfer for every model is the same.

coarse resolved scales (modes with wavenumber less than $k_c^h/2$) is a very small fraction of the total energy transfer. Most of the energy transfer to the subgrid scales is from modes with wavenumbers close to the cut-off k_c^h . This observation is consistent with the picture of local energy transfer in wavenumber space reported by several researchers (see also Figure 1).

In the third column of Table 1, we have reported the ratios of energy transfer implied by the Smagorinsky model. These values have been obtained by using (3.2), (3.4) and (3.5) in (2.18) and (2.19). We observe that this model predicts a more equal transfer from the coarse and the fine scales, which is in conflict with true transfer. This observation may be interpreted as a motivation for the variational multiscale approach (Hughes, Mazzei & Jansen 2000; Hughes, Mazzei, Oberai & Wray 2001), which involves applying the Smagorinsky model to the fine scales and applying no model to the coarse scales (see Figure 1).

3.2. Finite Element Basis

We expand the DNS solution and its restrictions to finite dimensional spaces using typical finite element basis functions. In particular, we use shape functions with trilinear interpolation. We utilize an equal number of grid points in each direction. The space \mathcal{V} is spanned by N^3 such functions. Likewise \mathcal{V}^h is spanned by $(N^h)^3$ functions, with

$N^h \ll N$. The restriction operator \mathcal{P}^h is the nodal interpolant of \mathcal{V} onto \mathcal{V}^h . As a result

$$\mathbf{U}(\mathbf{x}) = \sum_{a,b,c=1,2,\dots}^N \mathbf{U}(x_a, y_b, z_c) \phi_a^\delta(x) \phi_b^\delta(y) \phi_c^\delta(z) \quad (3.6)$$

$$\mathcal{P}^h \mathbf{U}(\mathbf{x}) = \sum_{a,b,c=\alpha,2\alpha,\dots}^N \mathbf{U}(x_a, y_b, z_c) \phi_a^h(x) \phi_b^h(y) \phi_c^h(z) \quad (3.7)$$

$$\mathbf{V}^h(\mathbf{x}) = \sum_{a,b,c=\alpha,2\alpha,\dots}^N [\mathbf{u}, 0]^T(x_a, y_b, z_c) \phi_a^h(x) \phi_b^h(y) \phi_c^h(z), \quad (3.8)$$

where δ is the mesh size associated with the DNS solution and h is the mesh size associated with the ideal LES solution. The ratio $\alpha = N/N^h$ and

$$\phi_a^h(\xi) = \begin{cases} (x - x_a + h)/h, & x \in (x_a - h, x_a) \\ (x_a + h - x)/h, & x \in (x_a, x_a + h) \\ 0, & \text{otherwise.} \end{cases} \quad (3.9)$$

To be consistent with the spectral case we select $N = 512$ and $N^h = 64$, which implies $\alpha = 8$.

Using (3.6), (3.7) and (3.8) in (2.12) we compute the net energy transferred to the subgrid scales. In this case, in contrast to the spectral case, the contribution from the linear terms in the Navier-Stokes equations is not zero. However we have verified that it accounts for only about 10% of the total transfer. Hence, most of the subgrid transfer is due to the nonlinear term in the Navier Stokes equation. Based on this observation we now compute the proportion of this transfer from the coarse and fine resolved scales.

In order to compute the multiscale transfer of energy we define $\bar{\mathcal{V}}^h$ to be the space spanned by shape function of mesh size $2h$. The dimension of this space is $(N^h/2)^3$ and

$$\bar{\mathbf{V}}^h(\mathbf{x}) = \sum_{a,b,c=2\alpha,4\alpha,\dots}^N [\mathbf{u}, 0]^T(x_a, y_b, z_c) \phi_a^{2h}(x) \phi_b^{2h}(y) \phi_c^{2h}(z) \quad (3.10)$$

$$\hat{\mathbf{V}}^h(\mathbf{x}) = \mathbf{V}^h(\mathbf{x}) - \bar{\mathbf{V}}^h(\mathbf{x}). \quad (3.11)$$

Using (3.6), (3.7), (3.10) and (3.11) in (2.16) and (2.17) we compute the energy transfer from the coarse and fine resolved scales. The values of the multiscale transfers are reported in the second column of Table 1. We observe that the energy transferred to the subgrid scales exclusively from the coarse resolved scales is a now a significant proportion of the total energy transfer. It is in fact greater than the energy transfer to the subgrid scales from the fine resolved scales. This picture is very different from the Fourier case, where the transfer from the fine resolved scale is seen to dominate.

In the fourth column of Table 1, we have also reported the transfer predicted by the Smagorinsky model, obtained by using (3.7), (3.10) and (3.11) in (2.18) and (2.19). We observe that in this case the ratios of transfer predicted by the Smagorinsky model are closer to the ideal values. Furthermore the multiscale approach of removing the Smagorinsky model from the coarse scales does not appear to be warranted.

| | Numerical Estimate for Ideal Model | | Numerical Estimate for Smagorinsky | | Analytical Estimate for Ideal Model | |
|-----------------|---------------------------------------|------|---------------------------------------|------|----------------------------------------|------|
| | Fourier | FEM | Fourier | FEM | Fourier | FEM |
| \bar{T}^h/T^h | 0.04 | 0.65 | 0.30 | 0.42 | 0.25 | 0.49 |
| \hat{T}^h/T^h | 0.96 | 0.35 | 0.70 | 0.58 | 0.75 | 0.51 |

TABLE 1. Estimates of the ratios of multiscale transfer of energy due to the subgrid term.

4. Explanation of the Transfer

We now explain the numerical results of the previous section. Our analysis is based on the EDQNM analysis (see Kraichnan 1976; Leslie & Quarini 1979). We first consider the spectral case and then the finite element case.

4.1. Spectral Basis

In Leslie & Quarini 1979 the authors have reported the subgrid spectral viscosity $\nu_n(k)$ corresponding to the sharp cut-off filter. Their results appear in Figure 2 of Leslie & Quarini 1979. Once this viscosity is known, the transfer between any two wavenumbers k_1 and k_2 is estimated by evaluating $T(k_1, k_2) = 2 \int_{k_1}^{k_2} \nu(k) k^2 E(k) dk$, where $E(k) = K_o \epsilon^{2/3} k^{-5/3}$. It may be easily verified that in the spectral case, the coarse and the fine scale energy transfers we wish to compute are given by $\bar{T}^h = T(0, k_c^h/2)$ and $\hat{T}^h = T(k_c^h/2, k_c^h)$. Using these expressions, and reading off the value of the spectral eddy viscosity from the figure, we numerically compute $\bar{T}^h/T^h = 0.25$ and $\hat{T}^h/T^h = 0.75$. These results once again indicate that the transfer is dominated by interactions that are local in the wavenumber space. Note that this estimate is obtained for a spectrum with an infinite inertial range. When the spectrum is flatter than $k^{-5/3}$ in the low wavenumbers and steeper than $k^{-5/3}$ in the high wavenumbers, as it must be for any realistic problem, the plateau in the eddy viscosity is lowered. The net result then is that the transfer from the coarse modes is further reduced.

4.2. Finite Element Basis

To understand the energy transfer within the finite element basis using a similar approach, we take the Fourier transform of (3.7). This yields

$$\widehat{\mathcal{P}^h \mathbf{U}}(\mathbf{k}) = \sum_{a,b,c=\alpha,2\alpha,\dots}^N \mathbf{U}(x_a, y_b, z_c) \widehat{\phi}_a^h(k_x) \widehat{\phi}_b^h(k_y) \widehat{\phi}_c^h(k_z), \quad (4.1)$$

where $\widehat{\phi}_a^h$, which denotes the Fourier transform of ϕ_a^h , is obtained from (3.9) and is given by

$$\widehat{\phi}_a^h(k_x h) = \frac{2\pi}{N^h} e^{ik_x x_a} b(k_x h), \quad (4.2)$$

where

$$b(\eta) = \frac{2(1 - \cos \eta)}{\eta^2}. \quad (4.3)$$

Utilizing (4.2) in (4.1) we arrive at

$$\widehat{\mathcal{P}^h \mathbf{U}}(\mathbf{k}) = \left[\left(\frac{2\pi}{Nh} \right)^3 \sum_{a,b,c=\alpha,2\alpha,\dots}^N \mathbf{U}(x_a, y_b, z_c) e^{i(k_x x_a + k_y y_b + k_z z_c)} \right] b(k_x h) b(k_y h) b(k_z h) \quad (4.4)$$

In the equation above, the term within the square brackets represents the Fourier coefficients of \mathbf{U} , evaluated using a finite, uniform quadrature rule. Replacing these approximate Fourier coefficients with their exact values, we arrive at

$$\widehat{\mathcal{P}^h \mathbf{U}}(\mathbf{k}) = \hat{\mathbf{U}}(\mathbf{k}) b(k_x h) b(k_y h) b(k_z h). \quad (4.5)$$

From the equation above we conclude that $\mathcal{P}^h \mathbf{U}$ may be approximated by a filtered version of \mathbf{U} where the filter, represented by the tensor product involving b is anisotropic. However since we are dealing with isotropic turbulence, following Leslie & Quarini 1979, we may replace this filter (by inducing a small error) with its isotropic component. Thus we have,

$$\widehat{\mathcal{P}^h \mathbf{U}}(\mathbf{k}) = \hat{\mathbf{U}}(\mathbf{k}) G(kh), \quad (4.6)$$

where

$$G(kh) = (4\pi)^{-1} \int_{\Gamma} b(k_x h) b(k_y h) b(k_z h) d\Gamma. \quad (4.7)$$

In the equation above the integral is taken over all angular directions for a fixed k . Thus comparing (4.6) with (3.2) we conclude that the Fourier transforms of both the spectral and the finite element forms of $\mathcal{P}^h \mathbf{U}$ may be written in the general form given by (4.6) with different interpretations of the filter G . For the finite element case the filter is given by (4.7) and for the spectral case the filter is a sharp cutoff filter with a cutoff at $k = k_c^h$. Both these filters are plotted in Figure 2. In addition, in this figure we have also plotted the Gaussian filter and isotropic component of the top-hat filter described in Leslie & Quarini 1979.

In Figure 2, we observe that the filter implied by the finite element basis is a graded filter, much like the Gaussian and the top-hat filters. Thus based on the analysis presented in Leslie & Quarini 1979, for the finite element basis we expect an eddy viscosity that is similar to that for the Gaussian or the top-hat filters. This viscosity, which is plotted in Figure 3 in Leslie & Quarini 1979 is constant for $kh \in (0, 1)$ and thereafter reduces smoothly to zero. Beyond $kh > 2\pi$, it is almost zero. Assuming for now that the viscosity for the filter induced by the finite element shape functions is the same, we calculate the expected values of transfers T^h and \bar{T}^h . Recognizing that

$$\widehat{\mathcal{P}^h \mathbf{V}}(\mathbf{k}) = \hat{\mathbf{V}}(\mathbf{k}) G(2kh), \quad (4.8)$$

it may be verified that these transfers are given by

$$T^h = 2 \int_0^\infty \nu(k) k^2 E(k) G^2(kh) dk \quad (4.9)$$

$$\bar{T}^h = 2 \int_0^\infty \nu(k) k^2 E(k) G^2(2kh) dk \quad (4.10)$$

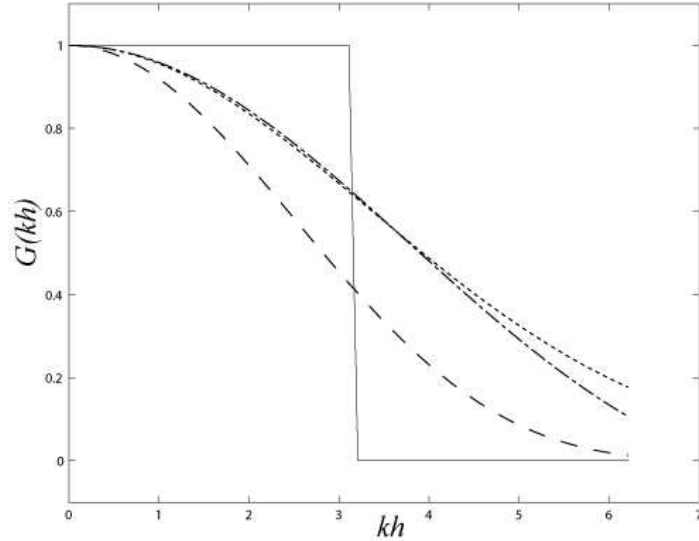


FIGURE 2. Plot of various Filters. Solid line: sharp cutoff filter; Dashed: Filter induced by the FEM basis; Dash-dot: Top-hat filter; Dotted line: Gaussian filter

$$\hat{T}^h = T^h - \bar{T}^h. \quad (4.11)$$

Once again assuming an infinite inertial range, we can explicitly calculate the ratios $\bar{T}^h/T^h = 0.49$ and $\hat{T}^h/T^h = 0.51$. Thus in this case we conclude that the transfer of energy from the coarse and the fine resolved scales is about the same. When compared with the spectral case, this increase in the contribution from the coarse scales for the finite element case, is consistent with the numerical results reported in Table 1.

5. Conclusions

In this manuscript we have performed an *a-priori* study of the transfer of energy from the resolved scales to the subgrid scales in the large eddy simulation of homogeneous isotropic turbulence. Our goal was to uncover the scale dependence of this transfer and the effect of the choice of an ideal resolved scale (LES) solution. In this regard, we found

(a) When the ideal LES solution is defined to have the same Fourier coefficients as the exact solution up to the cut-off wavenumber, then the energy transfer is predominantly from the fine resolved scales represented by modes that are close to the cutoff wavenumber.

(b) When the ideal LES solution is defined as the nodal interpolant of the exact solution on a typical finite element basis then the transfer from both the coarse and the fine resolved scales is significant.

We also analyzed the ability of the Smagorinsky model to replicate the transfer described above. We found that in spectral case the model is overly dissipative in the coarse scales, hence justifying the variational multiscale approach of Hughes, Mazzei, Oberai & Wray 2001. However, in the finite element case we found that the model performs reasonably well in imposing the right proportion of dissipation from the coarse and the fine

resolved scales. Thus indicating that in this case the multiscale modification does not appear to be warranted.

Finally, we provided a theoretical justification of our numerical observations based on the EDQNM closure. Using the results of Leslie & Quarini 1979, we demonstrated the dominance of the energy transfer from the fine resolved sales in the spectral case. In addition, we established that the ideal finite element solution could be obtained applying a graded filter to the exact solution. Thereafter, by assuming that the effective subgrid viscosity for this filter is the same as that of a Gaussian filter, we demonstrated that the energy transfer from the coarse resolved scales is significant.

REFERENCES

- CERUTTI, C., MENEVEAU, C. & KNIO, O.M. 2000 Spectral and Hyper Eddy Viscosity in High-Reynolds-Number Turbulence. *Journal of Fluid Mechanics*, **421**:307–338.
- COLLIS, S.S. 2001 Monitoring unresolved scales in multiscale turbulence modeling. *Physics of Fluids*, **13**(6):1800–1806.
- FOAIS, C., MANLEY, O., ROSA, R. & TEMAM, R. 2001 *Navier-Stokes Equations and Turbulence*. Cambridge University Press, Cambridge.
- HUGHES, T.J.R., MAZZEI, L. & JANSEN, K. E. 2000 Large Eddy Simulation and the Variational Multiscale Method. *Computing and Visualization in Science*, **3**:47–59.
- HUGHES, T. J. R., MAZZEI, L., OBERAI, A. A., & WRAY, A. A. 2001 The Multiscale Formulation of Large Eddy Simulation: Decay of Homogeneous Isotropic Turbulence. *Physics of Fluids*, **13**(2):505–512.
- HUGHES, T. J. R., OBERAI, A. A. & MAZZEI, L. 2001 Large Eddy Simulation of Turbulent Channel Flows by the Variational Multiscale Method. *Physics of Fluids*, **13**(6):1784–1799.
- JIMENEZ, J., WRAY, A. A., SAFFMAN, P. G. & RO GALLO, R. S. 1993 The Structure of Intense Vorticity in Isotropic Turbulence. *Journal of Fluid Mechanics*, **225**:65–90.
- KRAICHNAN, R.H. 1976 Eddy Viscosity in Two and Three Dimensions. *Journal of the Atmospheric Sciences*, **33**:1521–1536.
- LESLIE, D. & QUARINI, G. 1979 The Application of Turbulence Theory to the Formulation of Subgrid Modelling Procedures. *Journal of Fluid Mechanics*, **91**:65–91.
- SMAGORINSKY, J. 1963 General Circulation Experiments with the Primitive Equations. I. The Basic Experiment. *Monthly Weather Review*, **91**:99–164.